

# Driven nonlinear atomic force microscopy cantilevers: From noncontact to tapping modes of operation

Dror Sarid, Todd G. Ruskell, Richard K. Workman, and Dong Chen  
*Optical Sciences Center, University of Arizona, Tucson, Arizona 85721*

(Received 24 July 1995; accepted 27 November 1995)

A numerical model of the operation of an atomic force microscope with a driven cantilever is presented. This model takes into account the attractive van der Waals and repulsive indentation forces acting between tip and sample. The time-dependent displacement amplitude and phase of the tip oscillations, and the magnitude, duration, and sign of the short bursts of tip-sample force are derived. It is shown that the stiffness of the tip and sample materials is an important factor in determining the magnitude and duration of the tip-sample repulsive force and the magnitude of sample indentation. The model covers typical operating ranges of vibrating cantilever atomic force microscopes, from the noncontact to the tapping modes. © 1996 American Vacuum Society.

In a contact mode atomic force microscope (AFM),<sup>1,2</sup> the tip-sample force  $F$  is balanced by the force exerted by the deflection of the cantilever,  $z = F/k$ , where  $k$  is the cantilever spring constant. Operating in this mode can yield images of conducting as well as nonconducting samples with atomic resolution. To probe electric, magnetic, and atomic forces, the cantilever can be moved slightly away from the surface of the sample and vibrated at or near its resonance frequency.<sup>3-5</sup> For an amplitude of vibration much smaller than the tip-sample distance, one can use a perturbation approximation to model the influence of the tip-sample force on the mechanical properties of the vibrating cantilever. The approximation yields an effective spring constant,  $k_1 = k - F'$ , and a shifted resonance frequency  $\omega_1 = [k_1/m]^{1/2}$ .<sup>3</sup> Here,  $m$  is the cantilever effective mass and  $F'$  is the local tip-sample force derivative that changes the free-standing angular resonance frequency from  $\omega_0$  to  $\omega_1$ . This change in resonance frequency gives rise to a change in the phase and amplitude of the cantilever, which can then be used to obtain the force derivative. By mounting the cantilever on a piezoelectric element and employing a feedback system, one can get a topographic map of force derivatives that originate either from the true topography or from electric or magnetic forces across the surface of a sample. The disadvantage of operating in this so-called noncontact mode is some loss in resolution, while the advantage is that a substantial increase in sensitivity to small force derivatives can be obtained.<sup>3-7</sup> However, atomic resolution can still be obtained if the apex of the vibrating tip is close enough to the probed surface at its lowest point.<sup>8</sup>

The perturbation approach used to model the noncontact mode works well only for small amplitudes when the tip is far away from the surface. When the amplitude of vibration is such that the tip encounters a large variation in the force derivative, the approximation fails completely, and one has to solve the equation of motion of the cantilever numerically. In this article, we present a method to solve this equation of motion and use the solution to calculate the tip-sample force. The proposed method eliminates noise associated with the well-known problem of a driven nonlinear oscillator.<sup>9</sup>

The attractive force used here consists of a sphere-plane 2-8 van der Waals type force derived from an integration of the 6-12 force.<sup>10</sup> At a particular tip-sample distance, denoted by  $z_0$ , the force turns from attractive to repulsive. For distances  $z < z_0$ , the spherical tip pushes against the surface of the sample, and deforms it. A classical indentation force can then be used to model this repulsive part of the tip-sample interaction. We have used a combination of these two forces for the analysis of the vibration of the tip and the force it exerts on the surface of the sample. Although such a combination is only an approximate picture of the true forces, it makes it possible to obtain a clearer understanding of the operation of a tapping mode atomic force microscope.

The analysis of the tip-sample interaction presented in this article is especially important for the tapping mode of operation, in which the vibrating tip is actually in contact with the sample for a small portion of each cycle. This mode of operation is useful because it eliminates the lateral forces acting on the tip of an AFM operating in the contact mode,<sup>11-18</sup> and in general offers improved resolution over the noncontact mode. This article demonstrates that one can use a rather simple model for estimating the tip-sample forces that can be applied to both the noncontact and tapping modes.

The Lennard-Jones type interaction for a sphere-plane system<sup>10</sup> assumes a tip with radius  $R$ , Hamaker constant  $H$ , and typical atomic size  $\sigma$  for the tip and flat sample. The acting force can be approximated by

$$F(z) = \frac{HR}{6\sigma^2} \left[ -\left(\frac{\sigma}{z}\right)^2 + \frac{1}{30} \left(\frac{\sigma}{z}\right)^8 \right]. \quad (1)$$

We will use Eq. (1) for tip-sample separations larger than  $z_0 = 30^{-1/6}\sigma$ , where the force vanishes. To model the repulsive force for  $z < z_0$ , we use a modified Hertz model<sup>19-22</sup> that yields a reasonable approximation to the deformation of two contacting spheres with radii  $R_i$ . According to this theory, the radius of contact of the two spheres  $a$  is given by

$$a^3 = \frac{3}{4} \pi (\kappa_1 + \kappa_2) \frac{R_1 R_2}{R_1 + R_2} F(z). \quad (2)$$

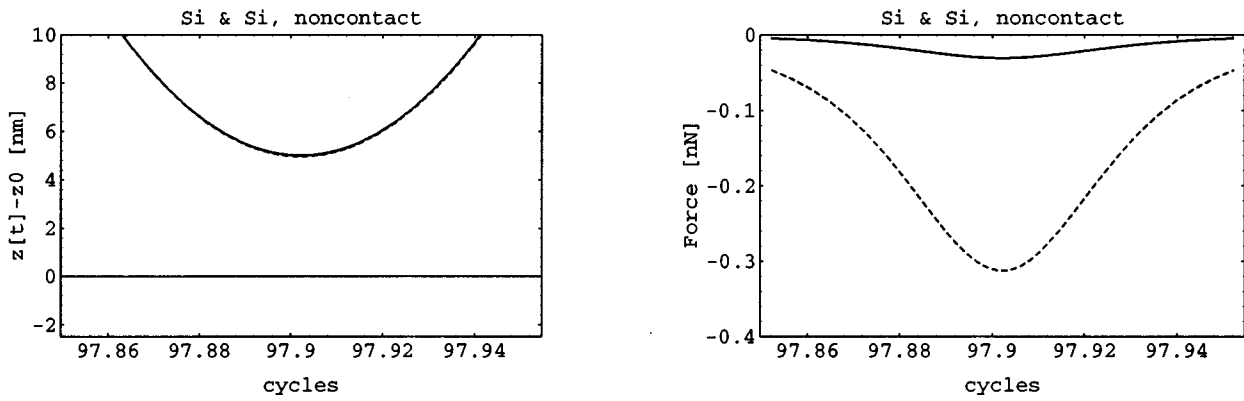


FIG. 1. The position of the tip,  $z(t) - z_0$  (left) and the force  $F(t)$  (right) for the noncontact mode. The solid and dashed lines refer to 5 and 50 nm radius tips, respectively.

Here,  $\kappa_i = (1 - \nu_i^2)/\pi E_i$ ,  $E_i$  is Young's modulus,  $\nu_i$  is Poisson's ratio, and  $F(z)$  is the applied force. Assume now that  $R_1 \ll R_2$ , namely, a sphere with  $E_1$  and  $R = R_1$  deforming a plane with  $E_2$ . A small indentation of the plane by  $|z - z_0| \ll R$  will result in an indentation radius  $a = \sqrt{2R(z - z_0)}$ . Inserting this value of  $a$  into Eq. (2) yields  $F(z) = g_0(z - z_0)^{3/2}$ , with

$$g_0 \equiv \frac{8\sqrt{2}}{3\pi(\kappa_1 + \kappa_2)} \sqrt{R}. \quad (3)$$

The equation of motion of the driven cantilever system is

$$m \frac{d^2 z}{dt^2} + m \frac{\omega}{Q} \frac{dz}{dt} + k[z(t) - z_1 - A \sin(\omega t)] - F[z(t)] = 0, \quad (4)$$

with the tip-sample force given by

$$F[z, (t)] = \begin{cases} \frac{HR}{6\sigma^2} \left[ -\left(\frac{\sigma}{z}\right)^2 + \frac{1}{30} \left(\frac{\sigma}{z}\right)^8 \right], & z > z_0 \\ g_0(z - z_0)^{3/2}, & z \leq z_0 \end{cases} \quad (5)$$

Here,  $Q$  is the quality factor of the free-standing vibrating cantilever, and  $m$  its effective mass given by  $m = k/\omega_0^2$ . It is useful to convert Eq. (4), which is a second-order differential equation in  $z(t)$ , into two first-order differential equations in  $z(t)$  and velocity  $v(t)$ . Convenient boundary conditions for these two first-order differential equations are  $z(0) = z_1$  and  $v(0) = 0$ . Namely, the cantilever is positioned at a set-point distance  $z_1$  from the sample with zero velocity. As the cantilever starts vibrating, its amplitude builds up to a maximum value of  $AQ$  unless the tip encounters an external force.

For the numerical simulations, we choose  $\sigma = 0.34$  nm,  $H = 10^{-18}$  J,  $\nu = 0.5$ ,  $E = 9$  GPa for a Langmuir-Blodgett (LB) film,<sup>21</sup> and 179 GPa for Si.<sup>5</sup> The corresponding  $g$  values for a Si tip with a radius of 50 nm, tapping on these two media, are  $0.98 \times 10^7$  and  $10^8$  [mks], respectively. Note that the particular choice of parameters is not very important in this simulation because the Lennard-Jones potential plays only a relatively minor role in the numerical results for stiff cantilevers having  $k = 20$  N/m. In addition, for the repulsive regime of operation, we choose a range of values for  $g$  that

covers most practical cases. Also chosen for the simulations are a resonance frequency of vibration of 100 kHz,  $Q = 20$ , a bimorph amplitude of vibration  $A = 10$  nm, and a driving frequency at the steepest slope of the resonance curve,  $\omega_c = \omega_0(1 - 0.35/Q)$ .

The displacement  $z[t]$ , which is readily obtained from the solution of the differential equations, contains all the information about the tip-sample interaction. To extract this information, we take the Fourier transform of  $z[t]$  from the 80th to the 100th cycle (after the vibrating cantilever reaches a steady state), and use the first five harmonics to construct an analytic approximation of the true displacement. The analytic function is then used to obtain the time-dependent tip-sample force.

To demonstrate the usefulness of the modeling approach, we present one example for the noncontact mode, and two examples for the tapping mode, using Si as the tip material, and a Si surface and an LB film as the sample materials.

The position of the tip,  $z(t) - z_0$ , and the associated force  $F(t)$  for the noncontact mode are shown in Fig. 1 on the left- and right-hand sides, respectively. Here,  $z_0$  is the distance where the van der Waals force is equal to zero, and the solid and dashed lines refer to  $R = 5$  (sharp) and 50 (dull) nm tips, respectively. Note that the attractive force is proportional to the product of the Hamaker constant and the tip radius. Therefore, choosing sharp or dull tips is equivalent to using the same tip with two different tip-sample Hamaker constants. The amplitude of vibration is found to be practically identical for both tips, since the cantilever has a large spring constant, yet the force exerted on each differs by a factor of 10, as expected.

In Fig. 2, the position of the tip,  $z(t) - z_0$ , and the associated force  $F(t)$  are shown for the sharp (solid line) and dull (dashed line) tips tapping on a Si surface. As expected, the dull tip penetrates less into the surface of the sample. Here, however, the force acting on the dull tip in the repulsive regime (positive force) is somewhat larger than that acting on the sharp tip. The reason is that the dull tip is stopped by the indentation faster than the sharp one, and therefore loses energy faster. The clear message here is that the meaningful

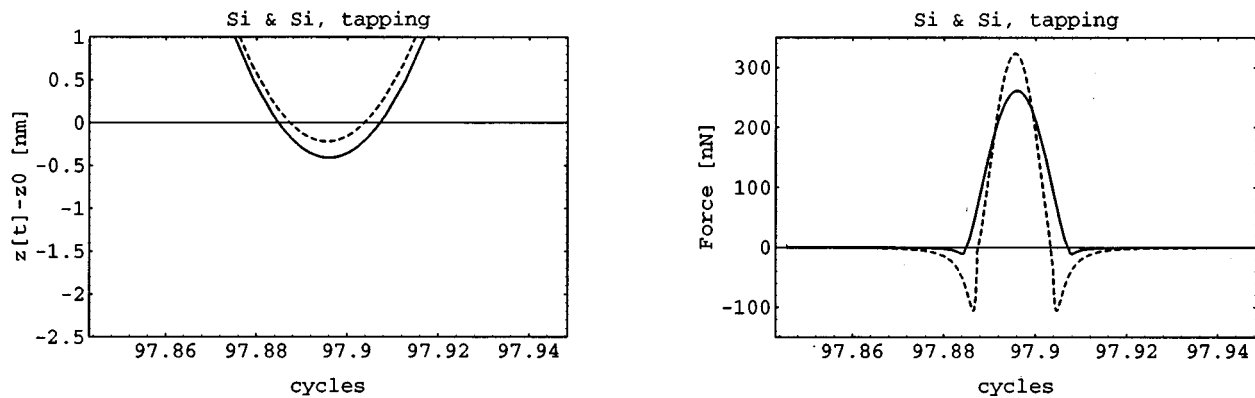


FIG. 2. The position of the tip,  $z(t)-z_0$  (left) and the force  $F(t)$  (right) for tapping with a Si tip on a Si surface. The solid and dashed lines refer to 5 and 50 nm radius tips, respectively.

measure for the tip-sample interaction, in the repulsive regime, is the pressure, rather than the force, and indeed we find for the sharp and dull tips that the maximum pressure is 21.3 and 4.73 GPa, respectively.

The position of the tip,  $z(t)-z_0$ , and the force  $F(t)$  are shown in Fig. 3 for the sharp (solid line) and dull (dashed line) tips tapping on an LB film. Here, the softer LB film experiences a larger indentation than does the Si sample, and the sharp tip penetrates deeper than the dull one. Again, the dull tip experiences a larger force than the sharp one, since it is stopped sooner. The maximum pressure here is 4.15 and 0.89 GPa for the sharp and dull tips, respectively.

In conclusion, we presented a model that yields the response of a vibrating cantilever for a range of set points covering the noncontact as well as the tapping modes of operation. For both of these modes, the user of the AFM can only monitor the amplitude and phase of the displacement, while the force has to be estimated from a given model that has to take into account the stiffness of the tip and sample and the tip-sample adhesion force. Note that the key differences between the noncontact and tapping modes are the

magnitude, duration, and sign of the tip-sample force pulses, while the tip is in close proximity to the sample. The main results derived from these figures are (a) for the noncontact mode, the sign of the force pulse is negative (attractive), small, and has a wide temporal profile; (b) for the tapping mode, the force pulse is mainly positive (repulsive), large, and has a narrow temporal profile; (c) in comparison to stiff samples, tapping on a soft sample yields a larger indentation, the force is weaker, and so is the pressure; (d) a sharp tapping tip exerts a smaller force, but a larger pressure on a sample than a dull tip; and (e) the pressure exerted by the tapping tip on a sample is a better measure of the tip-sample interaction than the force, as the pressure governs the magnitude of the indentation, and consequently the possible damage to the contacting surfaces.

*Acknowledgments:* The authors would like to acknowledge the support of the Air Force Office of Scientific Research, the National Science Foundation, and the Center for Microcontamination Control, University of Arizona. Helpful discussions with Yao Xiaowei are acknowledged.

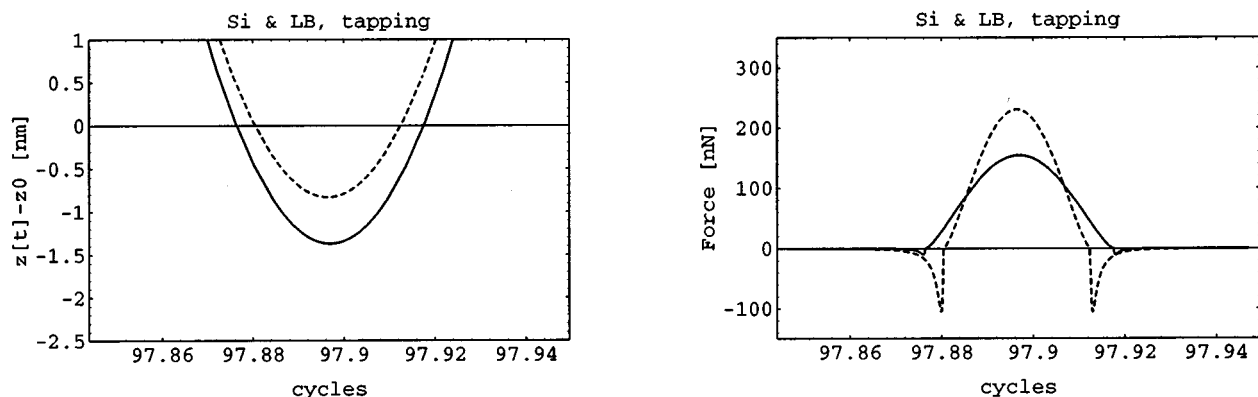


FIG. 3. The position of the tip,  $z(t)-z_0$  (left) and the force  $F(t)$  (right) for tapping with a Si tip on an LB film. The solid and dashed lines refer to 5 and 50 nm radius tips, respectively.

- <sup>1</sup>G. Binnig, C. F. Quate, and C. Gerber, *Phys. Rev. Lett.* **56**, 930 (1986).
- <sup>2</sup>G. Binnig, *Ultramicrosc.* **42–44**, 7 (1992).
- <sup>3</sup>Y. Martin, C. C. Williams, and H. G. Wickramasinghe, *J. Appl. Phys.* **61**, 4723 (1987).
- <sup>4</sup>G. M. McClelland, R. Erlandsson, and S. Chiang, *Scanning Tunneling Microscopy II*, edited by D. O. Thompson and D. E. Chimenti (Plenum, New York, 1987).
- <sup>5</sup>D. Sarid, *Scanning Force Microscopy*, revised ed. (Oxford University Press, New York, 1994).
- <sup>6</sup>*Scanning Tunneling Microscopy II*, edited by R. Wiesendanger and H.-J. Güntherodt (Springer, Berlin, 1992).
- <sup>7</sup>*STM and SPM in Biology*, edited by O. Mart and M. Amrein (Academic, San Diego, 1993).
- <sup>8</sup>F. J. Giessibl, *Science* **267**, 68 (1995).
- <sup>9</sup>S. H. Strogatz, *Nonlinear Dynamics and Chaos* (Addison-Wesley, New York, 1994).
- <sup>10</sup>J. N. Israelachvili, *Intermolecular and Surface Forces*, 2nd ed. (Academic, London, 1991).
- <sup>11</sup>Q. Zhong, D. Inness, K. Kjoller, and V. B. Elings, *Surf. Sci. Lett.* **290**, L688 (1993).
- <sup>12</sup>C. A. J. Putman *et al.*, *Appl. Phys. Lett.* **64**, 2454 (1994).
- <sup>13</sup>P. K. Hansma *et al.*, *Appl. Phys. Lett.* **64**, 1738 (1994).
- <sup>14</sup>R. Höper, R. K. Workman, D. Chen, D. Sarid, T. Yadav, J. C. Withers, and R. O. Loutfy, *Surf. Sci. Lett.* **311**, L731 (1994).
- <sup>15</sup>H. G. Hansma and J. H. Hoh, *Annu. Rev. Biophys. Biomol. Struct.* **23**, 115 (1994).
- <sup>16</sup>J. Chen, R. K. Workman, D. Sarid, and R. Höper, *Nanotechnol.* **5**, 199 (1994).
- <sup>17</sup>D. Sarid, J. Chen, and R. K. Workman, *Comp. Mater. Sci.* **3**, 475 (1995).
- <sup>18</sup>D. Sarid, *Comp. Mater. Sci.* (to be published).
- <sup>19</sup>K. L. Johnson, K. Kendall, and A. D. Roberts, *Proc. R. Soc. London Ser. A* **324**, 301 (1971).
- <sup>20</sup>S. R. Cohen, G. Neubauer, and G. M. McClelland, *Surf. Sci. Res. Rep.* **7205** (1989).
- <sup>21</sup>M. Radmacher, R. W. Tilman, and H. E. Gaub, *Biophys. J.* **64**, 735 (1993).
- <sup>22</sup>C. J. Chen, *Introduction to Scanning Tunneling Microscopy* (Oxford University Press, New York, 1993).